

# Calculating the vacancy formation energy in metals: Pt, Pd, and Mo

Thomas R. Mattsson and Ann E. Mattsson

*Surface and Interface Science Department, MS 1415, Sandia National Laboratories, Albuquerque, New Mexico 87185-1415*

(Received 5 August 2002; published 27 December 2002)

The predictive power of first-principles calculations of vacancy formation energies in metals (Pt, Pd, Mo) is improved by adding a correction for the intrinsic surface error in current implementations of density functional theory. The derived correction is given as a function of electron density; it can be explicitly applied to a wide range of systems. Density functional theory, contrary to claims in previous work, underestimates the vacancy formation energy when structural relaxation is included. This is the case whether using the local density- or the generalized gradient approximation for the exchange-correlation energy. With corrections for the intrinsic surface error we reach excellent agreement between calculated values using the two exchange-correlation functionals. Our final values for the three vacancy formation energies are 1.16, 1.70, and 2.98 eV for Pt, Pd, and Mo, respectively. The numbers are in good agreement with experimental data. We also calculate the barrier for vacancy diffusion in Pt to 1.43 eV.

DOI: 10.1103/PhysRevB.66.214110

PACS number(s): 61.72.Ji, 71.15.Mb, 73.90.+f

## I. INTRODUCTION

Atomic scale simulation without adjustable parameters can now be used as a tool for understanding experiments as well as an independent source of knowledge. Because there are many successful calculations in the literature analyzing various properties of materials, good agreement between density-functional-theory (DFT) (Ref. 1) calculations and experimental results is today, more or less, taken for granted.

However, DFT is not as reliable as one might imagine, even for systems as apparently simple as a monovacancy in fcc Pt or Pd. We show here that there is a large discrepancy between results for the vacancy formation energy from density-functional-theory calculations and experimental data. We also point out the origin of the discrepancy and calculate a crude correction for the error.

### A. Vacancies in metals

Vacancy migration is the dominant mechanism behind atomic transport, i.e., self-diffusion, in most elemental crystals, and is of fundamental importance in processes like solid phase transformations, nucleation and defect migration. Vacancies also play an important role for surface morphology, as shown very recently.<sup>2,3</sup>

Vacancies, created at the surface or at defects, exist at a certain concentration in all materials, depending exponentially on the formation energy of the vacancy and the temperature. That is, the equilibrium concentration  $c$  of vacancies is governed by the formation energy  $E_f$ ,

$$c \propto e^{(-E_f/k_B T)}, \quad (1)$$

where  $T$  is the temperature and  $k_B$  is Boltzmann's constant. The self diffusion coefficient is given by a similar expression

$$D \propto e^{-(E_f+E_m)/k_B T}, \quad (2)$$

where  $E_m$  is the migration energy (or diffusion barrier). The entropy of formation, as well as that of migration, also enters these expressions but the most important term, in particular at low temperature, is the energy.

Given the importance of vacancies, calculation of formation energies has been a natural subject of theoretical studies. Furthermore, the exponential dependence on the formation energy in Eqs. (1) and (2) makes it necessary to calculate the formation energy to high accuracy. A theoretical accuracy in energy of the order 0.025 eV is desired if rate predictions are to be made within a factor of three for processes occurring at room temperature ( $300k_B = 0.026$  eV).

When calculating energy differences it is helpful to remember the rule of thumb: "always try to compare similar systems." The bulk and the vacancy systems differ by the introduction of a void in the system. There is an exposed surface area in the case of a vacancy and not in the bulk case, resulting in a qualitative difference between the perfect bulk and vacancy systems, in turn increasing the demands of applicability on any theoretical method used. In order to improve the accuracy of DFT, attention has recently been devoted to the ability of different exchange-correlation functionals to treat systems with surfaces.<sup>4-6</sup> We will show how including these surface aspects of DFT helps in understanding results for vacancy formation energies.

In this paper we discuss Pt, Pd, and Mo. There are two reasons to study Pt: first, it has a large electron density, and we therefore expect<sup>4</sup> to reveal a large discrepancy between straightforward DFT calculations and experimental data. Second, there are recent experiments on the vacancy effect on Pt surface morphology.<sup>3</sup> Pd has the same density of electrons as Pt. So if the expectation for Pt regarding the surface correction is correct, Pd should also show similar behavior. In addition to these fcc metals we chose to study Mo, a bcc metal with a high melting temperature, for which there exist previous DFT calculations,<sup>7-9</sup> in addition to experimental work<sup>10,11</sup>.

Earlier calculations of the vacancy formation energy of these metals (not from first principles), include the works of Rosato *et al.*:<sup>12</sup> 1.28 and 1.0 eV for Pt and Pd, respectively; and Krause *et al.*:<sup>13</sup> 1.6 and 3.67 eV for Pt and Mo. The first *ab initio* calculation of the vacancy formation energy was made by Korhonen, Puska, and Nieminen (KPN) (Ref. 14) in 1994. They used DFT in the local density approximation (LDA) and treated the wave functions with full-potential

(FP) linearized muffin tin orbitals (LMTO's). Computational resources at that time did not allow for large systems or relaxation of transition-metal geometries. They consequently did not relax the systems and used a unit cell of 32 atoms. Their values for the vacancy formation energy of Pt, Pd, and Mo are 1.45, 1.65, and 3.13 eV. Somewhat surprisingly, considering the lack of relaxation and rather small unit cells, the values by KPN are rather close to the experimental values from positron annihilation measurements 1.35, 1.85, and 3.0 eV.<sup>10</sup>

Structural relaxation was included by Meyer and Fähnle<sup>7</sup> in their pseudopotential (PP) mixed-basis study of Mo, reporting a vacancy formation energy of  $2.9 \pm 0.1$  eV. Later, Korzhavyi *et al.*<sup>15</sup> made calculations based on the atomic sphere approximation (ASA) and a Green's-function method. They obtained 1.21, 1.43, and 2.50 eV for the vacancy formation energy of the three elements; the larger effective size of the supercells in the Green's-function formulation and the volume relaxation both reduce the formation energies slightly compared to the results of KPN. The ASA has inherent problems with bcc metals, explaining the larger difference for Mo.

Very recently, Söderlind *et al.*<sup>8</sup> investigated bcc transition metals, using FP-LMTO as well as PP plane waves. For Mo, their results are 2.85–3.00 eV, depending on the basis set, essentially confirming the findings of Meyer and Fähnle. In addition, Hoshino *et al.*<sup>9</sup> investigated, among other metals, Pd and Mo using a FP-KKR (Korringa, Kohn, and Rostoker) method and the generalized gradient approximates (GGA) for the exchange-correlation energy. Their results are 1.24 eV for Pd and 2.57 eV for Mo. That GGA gives lower values than the corresponding LDA calculations of KPN is expected.

However, none of the previous investigations of Pt and Pd included nuclear position relaxation. We will show in this paper that it is crucial to include structural relaxation also for these elements and that the previously reported agreement between unrelaxed LDA calculations and experimental results is fortuitous, a result of the cancellation of two unrelated effects.

## B. Outline of the paper

The outline of this paper is as follows: We first confirm the results of above mentioned work for the case of calculations without ionic relaxation (LDA), with unprecedentedly large supercells. Second, we allow for the relaxation of the system and quantify it. We then redo the calculations using the GGA exchange-correlation (XC) functional PW91.<sup>16</sup> Next, we estimate corrections for the intrinsic error that the LDA and GGA make at surfaces, and add them to the fully relaxed calculated values for the vacancy formation energy. Finally, we calculate the vacancy migration energy for Pt, and, via Eq. (2), show that the results for the vacancy formation energy and the migration barrier for Pt are inconsistent with experimental data unless the correction for the intrinsic surface error is taken into account.

## II. METHOD

Formally, DFT is an exact description of the ground state total energy and the electronic structure of a material. The

TABLE I. Convergence test for size of the Pt cell. Static: vacancy energy for a fixed lattice constant of 3.90 Å, no volume relaxation, the lattice constant is not the optimal one, the energies are therefore written within parentheses. Relaxed: full volume and geometrical relaxation. The finite size effects on the electronic structure is small for the 125-atom cell. The finite-size effect for unrelaxed systems is for Pt significantly smaller than the effect of structural relaxation. The 64-atom cell is large enough to allow for the most important relaxation to take place.

Cell size	$E_{\text{LDA}}^{\text{static}}$ (eV)	$E_{\text{LDA}}^{\text{relax}}$ (eV)	$E_{\text{GGA}}^{\text{relax}}$ (eV)
27	(1.28)		
64	(1.25)	0.99	0.72
108	(1.22)		
125	(1.21)	0.95	0.68

many-body Schrödinger equation is replaced by a set of effective single-particle equations, known as the Kohn-Sham equations.<sup>1</sup> The (unknown) many-body interaction is put into a separate term in the equations, the so called exchange-correlation functional/potential. This term is always approximated, for example in the local-density approximation.<sup>1</sup> The choice of exchange/correlation functional is the only physical approximation in the theory.

## A. Implementation and calculational details

The DFT calculations reported here were done with VASP.<sup>17</sup> The Kohn-Sham equations<sup>1</sup> are solved in a plane-wave basis set. The ions are described using ultrasoft pseudopotentials<sup>18</sup> (USP's). We use both the local density functional<sup>1</sup> and the PW91 functional<sup>16</sup> for exchange correlation. The accuracy of today's pseudopotentials is very good, when comparing the present unrelaxed results with the available FP-calculations (KPN and Hoshino *et al.*) we find the expected agreement for all three metals.

Cutoff energies used for the plane wave coefficients are: 191 eV for Pt, 249 eV for Pd, and 233 eV for Mo. The Brillouin zone is sampled using  $4 \times 4 \times 4$  mesh of  $k$  points for the 64- and 108-atom cells and a  $3 \times 3 \times 3$  mesh for the 125-atom cells. Given the size of the system in real space and the USP's, these choices ensure that the electronic structure is converged. The final convergence parameter is the size of the unit cell. Table I shows the results for Pt. The most important relaxation is included already in the 64-atom cell. We also conclude that the largest remaining error stems from the choice of XC potential.

The formation energy for the vacancy is calculated from

$$\Delta E = E_{\text{vac}} - \frac{n-1}{n} E_{\text{bulk}}, \quad (3)$$

where  $E_{\text{vac}}$  is the total energy of the cell containing a vacancy,  $n$  is the number of atoms in the bulk cell, and  $E_{\text{bulk}}$  denotes the total energy for a bulk calculation using the same cell and parameters. For the relaxed geometries we calculated the total energy for several volumes and found the minimum by fitting. Also, unrelaxed vacancy geometries are calculated at different volumes.

Finally, the minimum energy path for Pt vacancy migration, including the barrier, was calculated with the “nudged elastic band” method.<sup>19</sup> This is a straightforward way to calculate barriers when the initial and final geometries are known. We use four images, and spline interpolation, taking into account the energy as well as the forces, along the chain.<sup>20</sup>

### B. Estimate of the surface intrinsic error

As mentioned in Sec. I, the LDA and GGA make errors at surfaces. Fortunately, the errors per unit area are known. From exact surface exchange energies of Pitarke and Eguiluz<sup>21</sup> and “exact” RPA+ surface correlation energies of Yan *et al.*<sup>22</sup> for the jellium surface, we construct a reference system for use in the correction scheme presented in Ref. 6. LDA and PBE data for (identical) jellium surfaces are published in Refs. 4 and 23. From these data we have defined and parametrized a correction, per unit area, for the surface intrinsic error. When combined with the area of the exposed surface, an energy correction is readily calculated.

Reference 6 showed how to correct the surface intrinsic error resulting from an approximation to DFT in a real system. The idea is to use appropriate exact results for the surface exchange-correlation energy,  $\sigma_{xc}$ , for a reference system,

$$\Delta\sigma'_{xc} = \sigma'_{xc,ref}{}^{\text{exact}} - \sigma'_{xc,ref}, \quad (4)$$

where the prime stands for the type of exchange-correlation functional used. The correction is different for different functionals, although the two GGA versions PW91 and PBE are similar enough to use the same correction.

In Ref. 6 an exponential model with two parameters was used as a reference system for the exchange part of the energy. The two parameters were fitted to the real system. In order to obtain the required accuracy in the present treatment we must also include the correlation energy. This fact makes us choose a different reference system, the jellium surface, where “exact” data are available for both exchange and correlation. The jellium system has one parameter that can be used to map a real system to the reference system. The parameter is the bulk density of the jellium surface model.

There is a tradeoff between a good mapping of a real system onto the reference system and obtaining corrections for both exchange and correlation. If better mapping is required, surface correlation energies for a more useful reference system (such as the exponential model) need to be calculated. We have found, though, that real system surface profiles are similar to jellium surface profiles,<sup>24</sup> as can also be seen in Fig. 3 of Ref. 5.

Interpolating the jellium surface data is straightforward, but in many applications energies need to be extrapolated. Here we derive a interpolation/extrapolation scheme that is accurate over the full range of locally occurring bulk densities in real systems. The scheme is compared with a correction straightforwardly extracted from the interpolation/extrapolation formulas for the total surface exchange-correlation energy within the LDA, the PBE and “exact” work (based on the same data we use here) of Almeida,

Perdew, and Fiolhais (APF).<sup>23</sup> We use the numbers presented in Ref. 4 because the exchange and correlation energies are given separately there.

The surface exchange energy in the exponential model can be written as a factor depending on the bulk density multiplied with one depending on the profile. This also transfers to the correction. The profile-dependent part varies  $\pm 8\%$  (28%) in the LDA (GGA) (Ref. 6) over the interval  $2 < \tilde{r}_s < 6$ , or equivalently  $0.007 < \bar{n} < 0.201$  ( $\text{\AA}^{-3}$ ), while the bulk-density-dependent factor varies with a factor of 27. The bulk density dependence is thus by far the most important one.

The bulk-density-dependent factor is connected to the uniform electron-gas exchange energy, and by extracting the corresponding bulk-density-dependent factor from the uniform electron-gas correlation energy the nonanalytical behavior of the surface correlation energy can also be extracted as a (pre)factor in the jellium surface data. In the exchange case the prefactor is (see Ref. 6, given in units of Hartree/bohr<sup>2</sup>,  $\tilde{r}_s = r_s/a_0$ ,  $a_0$  the Bohr radius)

$$\sigma_{x,u}(\tilde{r}_s) = \frac{9}{16\pi^2\tilde{r}_s^3}, \quad (5)$$

and for the correlation it is

$$\sigma_{c,u}(\tilde{r}_s) = \frac{3}{8\pi\left(\frac{9\pi}{4}\right)^{1/3}\tilde{r}_s^2} \left( \tilde{r}_s + 3 + 4(\tilde{r}_s)^{1/2} - \frac{0.08}{(\tilde{r}_s)^{1/2}} \right). \quad (6)$$

It is important for the correlation energy<sup>25</sup> of the uniform electron gas to agree with the exact low- $\tilde{r}_s$  limit while still having a reasonable metallic range  $\tilde{r}_s$  behavior. The Lindgren-Rosén<sup>25</sup> formula fulfills these requirements.

By fitting the exchange energy

$$\frac{(\sigma'_{x,ref}{}^{\text{exact}} - \sigma'_{x,ref})}{\sigma_{x,u}} \sim c_1 \tilde{r}_s^\alpha, \quad (7)$$

and similarly for correlation, for both the LDA and PBE, the correction’s main dependence on the profile is captured. The parameters  $\alpha$  obtained are  $\alpha_x^{\text{LDA}} = 0.283$ ,  $\alpha_x^{\text{PBE}} = 0.380$ ,  $\alpha_c^{\text{LDA}} = -0.246$  and  $\alpha_c^{\text{PBE}} = 1.112$ . The remaining dependence (see Fig. 1) is modeled by a cosine function except for the LDA exchange, for which a parabolic function results in a better overall fit.

The final correction formulas are (in Hartree/bohr<sup>2</sup>)

$$\begin{aligned} \Delta\sigma_x^{\text{LDA}}(\tilde{r}_s) &= \sigma_{x,u}(\tilde{r}_s) \tilde{r}_s^{\alpha_x^{\text{LDA}}} \\ &\times (-0.0249 - 0.00393\tilde{r}_s + 0.000526\tilde{r}_s^2), \end{aligned} \quad (8)$$

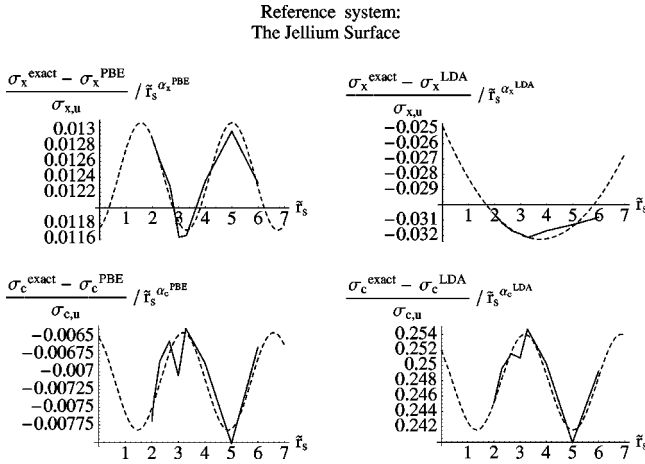


FIG. 1. Fitting of the remaining profile dependence for exchange (X) and correlation (C) for the LDA and PBE; see the text. Full line: exact data; dashed line: fit.

$$\Delta\sigma_x^{\text{PBE}}(\tilde{r}_s) = \sigma_{x,u}(\tilde{r}_s)\tilde{r}_s^{\alpha_x^{\text{PBE}}} \times [0.0124 + 0.000691 \cos(2.84 - 1.82\tilde{r}_s)], \quad (9)$$

$$\Delta\sigma_c^{\text{LDA}}(\tilde{r}_s) = \sigma_{c,u}(\tilde{r}_s)\tilde{r}_s^{\alpha_c^{\text{LDA}}} \times [0.248 - 0.00621 \cos(2.30 - 1.71\tilde{r}_s)], \quad (10)$$

$$\Delta\sigma_c^{\text{PBE}}(\tilde{r}_s) = \sigma_{c,u}(\tilde{r}_s)\tilde{r}_s^{\alpha_c^{\text{PBE}}} \times [-0.00714 - 0.000686 \cos(2.69 - 1.84\tilde{r}_s)]. \quad (11)$$

The individual exchange and correlation values are reproduced to less than 2 erg/cm<sup>2</sup> difference from the fitting data,

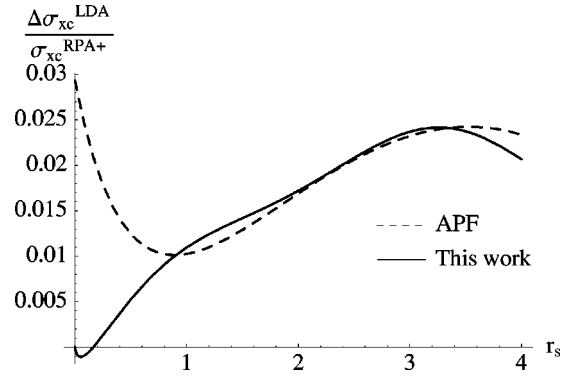


FIG. 2. Comparison between the relative LDA correction obtained by the extrapolation/interpolation formulas of Almeida, Perdew, and Fiolhais (APF) (Ref. 23), and the scheme in this work. In the slowly varying limit for the surface jellium system,  $r_s \rightarrow 0$ , the LDA approaches the exact value and the relative correction shall approach zero.

which is within the accuracy of the exact exchange and ‘‘RPA+’’ correlation numbers themselves. That the corrected LDA and corrected PBE numbers are the same, as seen in Table II, is the expected behavior.

In Figs. 2–4 we compare this interpolation/extrapolation scheme with the corresponding quantities obtained by the use of the APF extrapolation/interpolation schemes. In the slowly varying limit for the surface jellium system,  $r_s \rightarrow 0$ , the LDA and PBE, by construction, both approach the exact value, and the relative correction shall thus approach zero. Our parametrization behaves better than APF’s in this regime. Also the difference between LDA and PBE shall go to zero as  $r_s \rightarrow 0$ , Fig. 4 shows that in this respect our parametrization is also correct. A second advantage of the present formulation is that the exchange and correlation part of the energy can be corrected separately.

In Fig. 5, finally, the total (exchange and correlation) correction is presented as a function of bulk density. Figure 5 can be used to adjust any LDA or PBE/PW91 calculation with respect to the intrinsic surface error, the correction is not limited to vacancies.

TABLE II. Surface exchange-correlation energies, in erg/cm<sup>2</sup>, within the LDA and PBE and these values corrected according to the extrapolation/interpolation scheme presented here. The LDA and PBE values for  $\tilde{r}_s = 0.8$  and 1.0 are from Ref. 23 while the rest of these values are from Ref. 4, the same values we use as input in our extrapolation/interpolation scheme. Note that these latter values differ slightly from the values in Ref. 23. For comparison values obtained by the RPA+ and the RPA+ extrapolation/interpolation scheme presented in Table X of Ref. 23 are shown. Since corrected LDA and PBE give values very close to each other we believe that the RPA+ extrapolation/interpolation scheme gives too large values for small  $\tilde{r}_s$ , a trend that is also present in the corresponding extrapolation/interpolation schemes for LDA, PBE, and PKZB.

$\tilde{r}_s$	$\bar{n}$ (Å <sup>-3</sup> )	$\sigma_{xc}^{\text{LDA}}$	$\sigma_{xc}^{\text{PBE}}$	$\sigma_{xc}^{\text{LDA,corrected}}$	$\sigma_{xc}^{\text{PBE,corrected}}$	$\sigma_{xc}^{\text{RPA+}}$	$\sigma_{xc}^{\text{RPA+,*}}$
0.8	3.147	91 706	90 617	92 556	92 492		93 398
1.0	1.611	40 928	40 276	41 386	41 316		41 718
2.0	0.201	3 354	3 265	3 413	3 414	3413	3 414
3.0	0.060	764	743	783	783	781	782
4.0	0.025	261	252	267	267	268	268
5.0	0.013	111	107	113	113	113	113
6.0	0.007	53	52	56	55	54	54

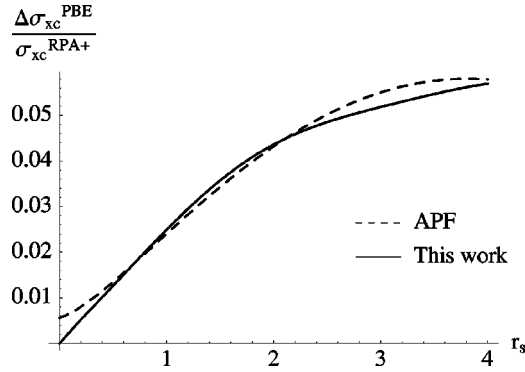


FIG. 3. Comparison between the relative PBE correction obtained by the extrapolation/interpolation formulas of Almeida, Perdew, and Fiolhais (APF) (Ref. 23), and the scheme presented in this work. Also the PBE approaches the exact result in the slowly varying limit for the surface jellium system,  $r_s \rightarrow 0$ .

With the corrections of Eqs. (8)–(11) the remaining property to calculate is thus the exposed surface area for vacancies in the different metals. To this end, we resort to scaling the vacancy area in Al, as determined in Ref. 5. The localized character of the  $d$  electrons makes it more difficult to estimate the exposed surface area in transition metals by fitting. By scaling the results for Al by the lattice constants we obtain a first estimation of the surface effect, without introducing additional fitting steps. The corrections are given in Table III.

### III. RESULTS

First we discuss the effects of structural relaxation and find that structural relaxation is important. Next, we calculate vacancy formation energies, including the correction for the intrinsic surface error. Finally, we present an analysis of the vacancy migration in Pt showing that the uncorrected values are inconsistent with each other and experimental data. Including the surface correction resolves this inconsistency.

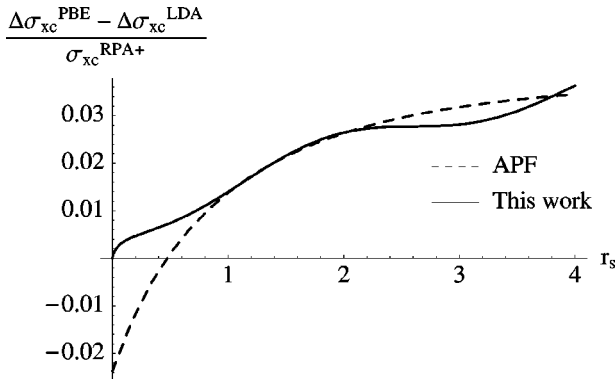


FIG. 4. The relative difference between PBE and LDA corrections obtained by the extrapolation/interpolation formulas of Almeida, Perdew, and Fiolhais (APF) (Ref. 23), and by the scheme presented in this work. In the slowly varying limit for the surface jellium system,  $r_s \rightarrow 0$ , the difference shall approach zero.

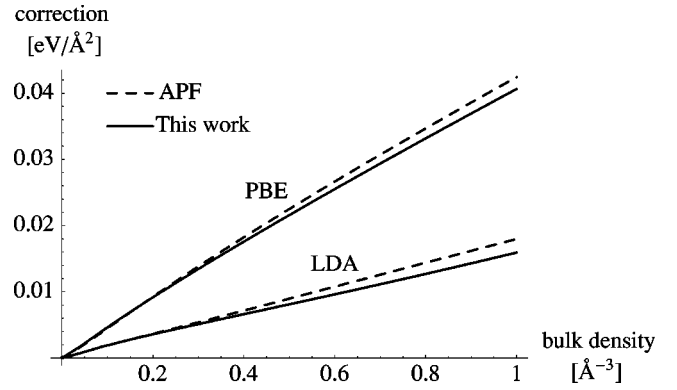


FIG. 5. The resulting correction as a function of the bulk density for LDA and PBE deduced from the extrapolation/interpolation formulas of Almeida, Perdew, and Fiolhais (APF) (Ref. 23), and by the scheme presented in this work. These corrections can be explicitly used to correct LDA and PBE/PW91 GGA calculations for the intrinsic surface error.

#### A. Effect of structural relaxation

Two kinds of relaxation are involved in a vacancy calculation: volume and structural relaxations. First a look at volume relaxation: a void causes electrons to partly fill it, to lower their kinetic energy. This rearrangement of electrons, in turn, reduces the density from the optimal bulk value in other parts of the system. Reducing the volume of the solid compensates for this effect. In calculations, this effect is large for small unit cells, since the reduction in bulk volume caused by the vacancy is a significant fraction of the cell volume. However, for large cells we find that this volume relaxation is irrelevant.

For Pt (LDA) the unrelaxed vacancy formation energies are 1.21, 1.31, and 1.38 eV for lattice constants 3.90, 3.91,

TABLE III. Surface intrinsic error for Al, Pt, Pd, and Mo for the local density (LDA) and generalized gradient (GGA) approximations of the exchange-correlation energy. The previously fitted radius for Al (Ref. 5) (1.2 Å) is used as references by scaling it with respect to the different lattice constants. In the case of Mo the radius is scaled with  $\sqrt{3/2}$  taking into account the difference in nearest neighbor distance in a bcc metal. The electron density is a function of the lattice volume and the number of electrons per unit cell. This treatment ignores the different vacancy formation volumes in different elements. For the fcc metals Pt and Pd this is not a source of error since the formation volume is 0.67 for Al (Ref. 5), very close to the vacancy formation volumes of Pd and Pt (0.68 and 0.69) (Ref. 15). The formation volume for bcc Mo is, on the other hand, slightly lower, 0.50 (Ref. 8). However, the decrease in area scales with  $r^2$ , not  $r^3$ . We estimate this effect as being less than 20% of the correction, that is 0.02 (0.06) eV in the LDA (GGA).

Element	$N_{\text{elect.}}$	$a_{\text{latt}}, (\text{Å})$	Bulk density, $\text{Å}^{-3}$	$\Delta E_{\text{LDA}}$ (eV)	$\Delta E_{\text{GGA}}$ (eV)
Al	3	4.04	0.182	0.06	0.15
Pt	10	3.91	0.669	0.20	0.50
Pd	10	3.85	0.701	0.21	0.50
Mo	6	3.15	0.384	0.11	0.29

TABLE IV. Vacancy formation energy for Pt, Pd, and Mo using the local density (LDA) and generalized gradient (GGA) approximations. For Pt and Pd the unit cell is 125 atoms; for Mo it is 128 atoms. Static: volume relaxation only; relax: volume and structural relaxation; corrected: relaxed results including correction for the DFT intrinsic surface error. Experimental data from different methods: positron annihilation measurements (Ref. 10), thermopower, thermal conductivity, thermal diffusivity, specific heat, as quoted by Kraftmakher (Ref. 11), see Sec. III D. All energies are in eV.

Element	$E_{\text{LDA}}^{\text{static}}$	$E_{\text{LDA}}^{\text{relax}}$	$E_{\text{LDA}}^{\text{corrected}}$	$E_{\text{GGA}}^{\text{static}}$	$E_{\text{GGA}}^{\text{relax}}$	$E_{\text{GGA}}^{\text{corrected}}$	Expt. (eV).
Pt	1.30	0.95	<b>1.15</b>	1.00	0.68	<b>1.18</b>	1.24, 1.32, 1.35, 1.45
Pd	1.66	1.50	<b>1.71</b>	1.32	1.20	<b>1.70</b>	1.5, 1.7, 1.85
Mo	3.01	2.89	<b>3.00</b>	2.78	2.67	<b>2.96</b>	1.6, 2.24, 3.0, 3.0, 3.6

and 3.92 Å. When including volume relaxation the vacancy formation energy is 1.30 eV, taken at the optimum lattice constants 3.911 and 3.907 Å for the bulk and vacancy, respectively. The unrelaxed value at 3.91 Å is 1.31 eV. The effect of the volume relaxation is less than 1%.

For Pd (LDA) the corresponding series is 1.50, 1.59, 1.69, and 1.77 eV for lattice constants 3.82, 3.84, 3.86, and 3.88 Å. The volume optimized vacancy formation energy is 1.67 eV. The optimal bulk lattice constant is 3.857 Å; an interpolation of the unrelaxed values gives 1.675 eV for the vacancy formation energy. The volume relaxation effect is again very small.

For Mo (LDA) we obtain 2.59, 2.92, 3.12, and 3.30 eV for lattice constants 3.07, 3.09, 3.11, and 3.13 Å. The volume optimized value is 3.014 eV for the vacancy formation energy. For the optimal bulk lattice constant 3.10 Å, the unrelaxed interpolated vacancy formation energy is 3.017 eV. The volume relaxation is also minute for Mo.

Structural relaxation, on the other hand, is a local effect: Removing an atom draws neighboring atoms toward the vacancy. The relaxation is significant for the first atoms but small already for the second and third shell of atoms surrounding the vacancy. Table IV shows that the relaxation energy is largest in Pt and smallest in Mo. We note that our fully relaxed value for Mo (LDA) is 2.89 eV, which agrees to 1.4% with the results of Söderlind *et al.*<sup>8</sup> (2.85 eV). We conclude that, compared to structural relaxation, volume relaxation is irrelevant for the large unit cells in this work.

### B. Vacancy formation energy

The main results of this work are the vacancy formation energies in Table IV. We make five observations in the table: First, structural relaxation can reduce the vacancy formation energy by more than 30%. It is therefore important to include structural relaxation when calculating vacancy formation energies from first principles. Second, the LDA consistently gives higher values for the vacancy formation energy than the GGA does, and the difference is significant, up to 30–40%. Third, the calculated, relaxed values, are consistently smaller than the measured. Fourth, the differences between the LDA and GGA vanish completely, for all three elements, when the intrinsic surface errors are corrected for. Fifth, the surface-corrected values are, for both the LDA and GGA, in agreement with the majority of available experimental data. As a final estimate of the vacancy formation energies for the

three elements we calculate the mean of the LDA and GGA numbers: 1.16, 1.70, and 2.98 eV for Pt, Pd, and Mo, respectively.

### C. Vacancy migration energy of Pt

The calculated energies (LDA) along the transition path for Pt vacancy diffusion are shown in Fig. 6, from which we observe that the barrier for diffusion is  $\Delta E_{\text{LDA}}^{\text{Pt}} = 1.43$  eV. Measurements of self-diffusion give, as shown in Eq. (2), the sum of the formation energy and the migration energy. Since we have calculated both quantities we can calculate the activation energy for self-diffusion by adding  $\Delta E_{\text{LDA}}^{\text{Pt}}$  to the uncorrected vacancy formation energies of Table IV: 0.95 eV. The result is 2.38 eV. When comparing with the measured activation energy by Neumann and Tölle, 2.64 eV,<sup>26,27</sup> it is clear that the error in the formation energy propagates to the activation energy for self-diffusion. This short exercise suggests that the barrier is calculated more accurately than the vacancy formation energy. The reason is that the barrier is calculated by comparing two more similar systems than when calculating the vacancy formation energy. Although the

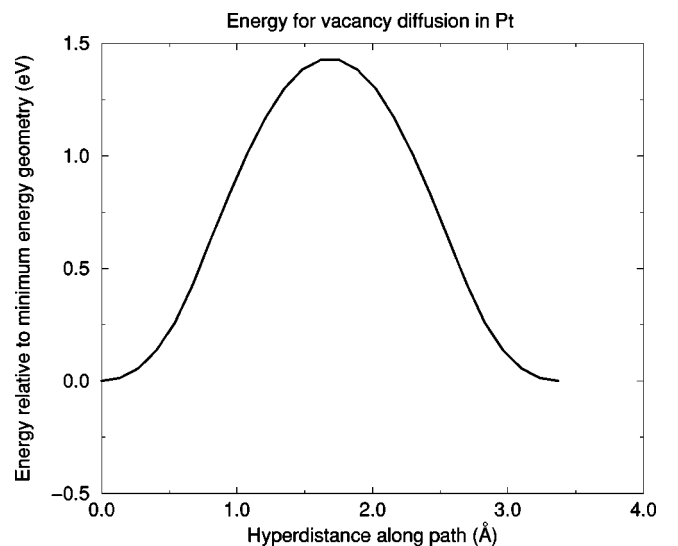


FIG. 6. LDA calculation of the reaction path for vacancy diffusion in Pt; the curve is a spline interpolation of four intermediate images in the chain. The forces are converged to 0.03 eV/Å on each degree of freedom. The barrier is 1.43 eV.

exposed surface area changes during the diffusion process, this change is smaller than the surface area introduced when creating a vacancy.

Nevertheless, the corrected vacancy migration energy can be calculated by estimating the difference in the exposed surface area between the transition state and the minimum-energy state.<sup>28</sup> The correction is 0.08 eV (less than the 0.20 eV for the vacancy formation energy) and the vacancy migration energy is  $1.51 \pm 0.02$  eV, with the estimated error stemming from two different models of the exposed area at the transition state. When adding the likewise corrected value for the formation energy in Table IV we obtain, for the activation energy for self diffusion in Pt (LDA),  $1.51 + 1.15 = 2.66$  eV, in excellent agreement with experiments.

#### D. Comparing with experimental data

The calculated vacancy formation energies are lower bounds to measured data for the vacancy formation energies. Simulations, for example of Al (Refs. 5 and 28), and Cu,<sup>29</sup> have shown that the formation enthalpy increases with temperature. In the case of Al the formation enthalpy changes from 0.69 to 0.78 eV from low temperature to the melting point. A first estimate of the effect is possible from straightforward thermodynamic considerations.<sup>11</sup> An increase in the vacancy formation energy as a function of temperature is expected for all elements.

There are many technical questions regarding the measurements of vacancies, and a critical discussion of the pros and cons of different techniques is well beyond the scope of this work. However, a few brief comments regarding different experimental approaches are necessary. The most important difference between various techniques is between equilibrium and nonequilibrium (quenching) experiments, with nonequilibrium experiments often harder to analyze due to the uncontrolled relaxation mechanisms active during quenching. A second major difference is that the vacancy concentration is very small at low temperatures, making measurements at low  $T$  difficult for techniques based on how bulk properties of materials change with the number of vacancies.

Positron annihilation experiments are widely regarded as the most important equilibrium technique at low  $T$ . The measurements are done in equilibrium and the theory of positron interaction with matter is mature.<sup>30</sup> At high  $T$ , measurements of heat capacity (specific heat), electrical resistivity, and differential dilatometry (thermal expansion not caused by the lattice but by increased number of vacancies), are the main techniques. The temperature dependence of the vacancy formation energy has been a subject of debate, in particular how to distinguish the lattice anharmonicity from the contributions of different point defects.<sup>11</sup> Often different experimental methods result in a large range of values. Assessing the reliability of the methods is a formidable task. Calculations from first principles provide additional independent information that can be used to evaluate experimental techniques. Given the agreement between the LDA and GGA, the large supercells, and the structural relaxation, we believe that the

present calculation can do that. Next we will, element by element, compare our calculated values with available experimental data.

Vacancies in Pt have been studied experimentally extensively (see Refs. 10 and 11 and references therein). The experimental number for the formation energy varies from 1.32 and 1.35 eV in positron measurements,<sup>10</sup> 1.6 eV (nonlinear specific heat at high  $T$ ) and 1.45 eV (thermopower), and 1.45 (thermal conductivity), to 1.3–1.7 eV (in different resistivity measurements), as quoted in Ref. 11. In addition, a temperature dependence analysis<sup>11</sup> of specific-heat data gives 1.24 eV for the formation energy at zero temperature deduced from the high- $T$  data. Our calculated numbers, including the correction for the intrinsic surface error, are 1.15 (1.18) eV for the LDA (GGA), thus slightly below the measured ones. For Pt, we conclude that the calculated numbers, the measured values from positron experiments, and the specific heat are in agreement. The other techniques all give numbers that are higher in energy, in agreement with the calculated numbers being a lower bound.

In the case of Pd there is less experimental data available. Positron annihilation reports 1.85 eV,<sup>10</sup> measurements of thermal conductivity 1.7 eV, and thermal diffusivity experiments 1.5 eV, as referenced in Ref. 11. Our calculated values are 1.71 (1.70) eV for the LDA (GGA). Since these numbers constitute a lower bound to the formation energy we contend that the thermal diffusivity measurements are low and a re-assessment of the measurements warranted.

Molybdenum is a bcc metal with high melting temperature and its vacancy formation energy has been reported in many studies. Positron measurements report 3.0, 3.0, and 3.6 eV,<sup>10,31</sup> resistivity 2.7–3.24 eV, and specific heat 2.24 eV, with 1.6 eV when extrapolated to zero temperature.<sup>11</sup> Our calculated values are 3.00 (2.96) eV for the LDA (GGA). Since our calculations are independent of experimental data, and by no means fitted to a particular type of experiments, we conclude that positron measurements are the preferred method to determine the vacancy formation energy in Mo.

#### IV. CONCLUDING REMARKS

We have shown that the historical quantitative agreement between DFT/LDA and experimental data for Pt and Pd is a result of cancellation of two *unrelated* effects. The importance of relaxation in vacancy calculations is clarified. When including relaxation as well as a correction for the intrinsic surface error, the results for vacancy formation and diffusion are internally consistent. The calculated vacancy formation energies are, for both the LDA and GGA, close to measured positron annihilation data.

Identifying the intrinsic surface error as an important factor in calculations of vacancy formation energies offers insight into DFT. In addition, the analysis improves our understanding of vacancies in metals, with the LDA and GGA giving similar results our ability to explain and predict vacancy properties becomes better. Vacancies in Al, Cu,<sup>5</sup> Pt, Pd, and Mo are all described well by structural relaxation and the correction for the intrinsic surface error. The detailed electronic structure of other bulk defects, like grain boundaries and dislocations, will govern whether the energy is af-

fectured by the correction or not. Other areas where the intrinsic surface error can play a role include surface energies, adhesion energies,<sup>24</sup> and wetting, growth and nucleation on surfaces, since adsorbate interaction and step energies can be affected, adsorption energies for molecules, and dissociation energies. Until functionals that correctly account for the evanescent character of wavefunctions at surfaces are developed, and widely used, this post-processing scheme offers a way to correct for the intrinsic surface error.

## ACKNOWLEDGMENTS

We thank Norman Bartelt, Peter Feibelman, Gary Kellogg, and Bene Poelsema for valuable discussions. T.R.M. acknowledges support from the Motorola/SNL computational materials CRADA. Sandia is a multiprogram laboratory operated by Sandia Corporation, a Lockheed Martin Company, for the United States Department of Energy under Contract DE-AC04-94AL85000.

- 
- <sup>1</sup>P. Hohenberg and W. Kohn, Phys. Rev. **136**, B864 (1964); W. Kohn and L. J. Sham, Phys. Rev. **140**, A1133 (1965).  
<sup>2</sup>K. F. McCarty, J. A. Nobel, and N. C. Bartelt, Nature (London) **412**, 622 (2001).  
<sup>3</sup>B. Poelsema, J. B. Hannon, N. C. Bartelt, and G. K. Kellogg (unpublished).  
<sup>4</sup>S. Kurth, J. P. Perdew, and P. Blaha, Int. J. Quantum Chem. **75**, 889 (1999).  
<sup>5</sup>K. Carling *et al.*, Phys. Rev. Lett. **85**, 3862 (2000).  
<sup>6</sup>A. E. Mattsson and W. Kohn, J. Chem. Phys. **115**, 3441 (2001).  
<sup>7</sup>B. Meyer and M. Fähnle, Phys. Rev. B **56**, 13 595 (1997).  
<sup>8</sup>P. Söderlind, L. H. Yang, John A. Moriarty, and J. M. Wills, Phys. Rev. B **61**, 2579 (2000).  
<sup>9</sup>T. Hoshino, T. Mizuno, M. Asato, and H. Fukushima, Mater. Trans., JIM **42**, 2206 (2001).  
<sup>10</sup>H. E. Schäfer, Phys. Status Solidi A **102**, 47 (1987).  
<sup>11</sup>Y. Kraftmakher, Phys. Rep. **299**, 79 (1998).  
<sup>12</sup>V. Rosato, M. Guillope, and B. Legrand, Philos. Mag. A **59**, 321 (1989).  
<sup>13</sup>U. Krause, J. P. Kuska, and R. Wedell, Phys. Status Solidi B **151**, 479 (1989).  
<sup>14</sup>T. Korhonen, M. J. Puska, and R. M. Nieminen, Phys. Rev. B **51**, 9526 (1995).  
<sup>15</sup>P. A. Korzhavyi *et al.*, Phys. Rev. B **59**, 11 693 (1999).  
<sup>16</sup>J. P. Perdew *et al.*, Phys. Rev. B **46**, 6671 (1992); **48**, 4978 (1993).  
<sup>17</sup>G. Kresse and J. Hafner, Phys. Rev. B **47**, 558 (1993); **49**, 14 251 (1994); G. Kresse and J. Furthmüller, *ibid.* **54**, 11 169 (1996).  
<sup>18</sup>D. Vanderbilt, Phys. Rev. B **41**, 7892 (1990); G. Kresse and J. Hafner, J. Phys.: Condens. Matter **6**, 8245 (1994).  
<sup>19</sup>G. Mills, H. Jónsson, and G. K. Schenter, Surf. Sci. **324**, 305 (1995).  
<sup>20</sup>Roland Stumpf (unpublished).  
<sup>21</sup>J. M. Pitarke and A. G. Eguiluz, Phys. Rev. B **63**, 045116 (2001).  
<sup>22</sup>Z. Yan, J. P. Perdew, S. Kurth, C. Fiolhais, and L. Almeida, Phys. Rev. B **61**, 2595 (2000).  
<sup>23</sup>L. M. Almeida, J. P. Perdew, and C. Fiolhais, Phys. Rev. B **66**, 075115 (2002).  
<sup>24</sup>A. E. Mattsson and D. R. Jennison, Surf. Sci. Lett. **520**, L611 (2002).  
<sup>25</sup>Ingvar Lindgren and Arne Rosen, Case Stud. At. Phys. **4**, 93-196 (1974); G. D. Mahan, *Many-Particle Physics* (Plenum Press, New York, 1990).  
<sup>26</sup>G. Neumann and V. Tölle, Philos. Mag. A **54**, 619 (1986).  
<sup>27</sup>G. Neumann and V. Tölle, Philos. Mag. A **61**, 563 (1990).  
<sup>28</sup>N. Sandberg, B. Magyari-Köpe, and T. R. Mattsson, Phys. Rev. Lett. **89**, 065901 (2002).  
<sup>29</sup>S. M. Foiles, Phys. Rev. B **49**, 14 930 (1994).  
<sup>30</sup>M. J. Puska and R. M. Nieminen, Rev. Mod. Phys. **66**, 841 (1994).  
<sup>31</sup>R. Ziegler and H. E. Schäfer, Mater. Sci. Forum **15-18**, 145 (1987).